



*euronoise*

**Acoustics'08  
Paris**  
June 29-July 4, 2008

[www.acoustics08-paris.org](http://www.acoustics08-paris.org)

## Unified and stable scattering matrix formalism for acoustic waves in piezoelectric stacks

Victor Zhang<sup>a</sup> and Vincent Laude<sup>b</sup>

<sup>a</sup>IEMN-CNRS, Av. Poincare, Cite Scientifique, B.P. 60069, 59652 Villeneuve d'Ascq Cedex,  
France

<sup>b</sup>Institut FEMTO-ST/CNRS, 32 avenue de l'Observatoire, 25044 Besançon cedex, France  
[victor.zhang@iemn.univ-lille1.fr](mailto:victor.zhang@iemn.univ-lille1.fr)

This paper presents the scattering  $\mathbf{s}$ -matrix formalism along with a stable recursive algorithm based on the total  $\mathbf{s}$ -matrix of a multilayered piezoelectric stack. By combining the  $\mathbf{s}$ -matrix and the surface impedance matrix of the external media, various terminations of the stack can be handled in a unified way. Numerical examples are given to show the functional features of the  $\mathbf{s}$ -matrix that are superior to other matrices. In addition to the unconditional stability throughout large and small thicknesses, the  $\mathbf{s}$ -matrix formalism is pole-free, branch point-sensitive, maintaining meanly-constant magnitude, keeping stable phase, and involving only dimensionless elements.

## 1 Introduction

Many matrix models have been proposed for numerical simulations of acoustic waves in piezoelectric stacked structures, including the well-known transfer  $\mathbf{T}$ -matrix [1-3], more recent hybrid  $\mathbf{H}$ -matrix [4], the impedance  $\mathbf{Z}$ -matrix [5-7] and its direct variant stiffness  $\mathbf{K}$ -matrix [8,9], as well as the scattering  $\mathbf{s}$ -matrix [10-14] comprising its partial form - reflection  $\mathbf{R}$ -matrix. Though the essential problems of the numerical stability with the  $\mathbf{T}$ -matrix are now resolved, numerical features of different matrix-based characteristic functions giving proper modes have not been systematically studied. We highlight the fact that for a problem of given *boundary conditions* (BC), the proper modes determined with any matrix formalism should be the same, but the form of the characteristic function is not unique. It varies with the formalisms used and can be formulated in different ways within the same formalism. With regard to functional behavior, the  $\mathbf{s}$ -matrix seems to have some interesting features superior to other matrices. Recently, we provided [14] a natural definition and a direct derivation of the  $\mathbf{s}$ -matrix for an elementary black-box containing a layer and an interface describing the linear relation of the amplitudes of waves entering and exiting the box, and developed a total  $\mathbf{s}$ -matrix-based full recursion algorithm for stacks of any finite number of boxes in terms of the  $\mathbf{s}$ -matrix of the last single box and the  $\mathbf{s}$ -matrix of the stack without the last box. The stack BC is formulated in versatile terms of the *surface impedance matrices* (SIM) of the external media. The stack BC and  $\mathbf{s}$ -matrix recursions are dealt with in parallel and independently one from another so that the stack recursion can be performed without specifying the stack BC and the same recursion results apply for different BC. In this paper, we investigate the numerical properties of the  $\mathbf{s}$ -matrix formalism and demonstrate its specific features: pole-free, unconditionally stable for both large and small frequency-thickness ( $f$  $h$ ) products, involving elements not only homogeneous but also dimensionless. The  $\mathbf{s}$ -matrix based characteristic functions are also shown to be branch point sensitive.

## 2 $\mathbf{s}$ -matrix and recursive algorithm

The *generalized interface scattering matrix* (GISM) of a black-box containing a single layer  $n$  of thickness  $h_n$  and an interface separating it with the next layer  $n+1$ , noted by  $\mathbf{S}^n$  of sub-matrices  $\mathbf{S}_{ij}^n$  ( $i,j=1,2$ ), is defined by

$$\begin{bmatrix} \mathbf{y}_{In}^- \\ \mathbf{y}_{Dn+1}^- \end{bmatrix} \equiv \begin{bmatrix} \mathbf{S}_{11}^n & \mathbf{S}_{12}^n \\ \mathbf{S}_{21}^n & \mathbf{S}_{22}^n \end{bmatrix} \begin{bmatrix} \mathbf{y}_{Dn}^- \\ \mathbf{y}_{In+1}^- \end{bmatrix} \quad (1)$$

( $x=D, I$ ) denote the wave amplitudes of the direct ( $D$ ) and inverse ( $I$ ) modes at the top ( $-$ ) and bottom ( $+$ ) surface of the layer  $n$ . The terms *Direct* and *Inverse* refers respectively to the positive and negative  $x_2$ -axis normal to the layering. The *generalized total scattering matrix* (GTSM) of the system containing  $m \geq 2$  boxes from  $n$  to  $n+m-1$ , noted by  $\mathbf{s}^{n,m}$ , is defined by

$$\begin{bmatrix} \mathbf{y}_{In}^- \\ \mathbf{y}_{Dn+m}^- \end{bmatrix} \equiv \begin{bmatrix} \mathbf{s}_{11}^{n,m} & \mathbf{s}_{12}^{n,m} \\ \mathbf{s}_{21}^{n,m} & \mathbf{s}_{22}^{n,m} \end{bmatrix} \begin{bmatrix} \mathbf{y}_{Dn}^- \\ \mathbf{y}_{In+m}^- \end{bmatrix}, m \geq 2. \quad (2)$$

Applying the state vector continuity at the interface assumed non metallized between any two adjacent layers in the layered structure, called stack, and after successively eliminating the intermediate mode amplitudes, we obtain the recursive relations for the GTSM  $\mathbf{s}^{n,m}$  of an  $m$ -box stack in terms of the GTSM  $\mathbf{s}^{n,m-1}$  of the stack without the last box and the GISM  $\mathbf{S}^{n+m}$  of the last single box [14]:

$$\mathbf{s}_{11}^{n,m} = \mathbf{s}_{11}^{n,m-1} + \mathbf{s}_{12}^{n,m-1} \mathbf{A}^{-1} \mathbf{S}_{11}^{n+m} \mathbf{s}_{21}^{n,m-1} \quad (3a)$$

$$\mathbf{s}_{12}^{n,m} = \mathbf{s}_{12}^{n,m-1} \mathbf{A}^{-1} \mathbf{S}_{12}^{n+m} \quad (3b)$$

$$\mathbf{s}_{21}^{n,m} = \mathbf{S}_{21}^{n+m} \mathbf{B}^{-1} \mathbf{s}_{21}^{n,m-1} \quad (3c)$$

$$\mathbf{s}_{22}^{n,m} = \mathbf{S}_{22}^{n+m} + \mathbf{S}_{21}^{n+m} \mathbf{B}^{-1} \mathbf{s}_{22}^{n,m-1} \mathbf{S}_{12}^{n+m} \quad (3d)$$

with  $\mathbf{A} \equiv \mathbf{I} - \mathbf{S}_{11}^{n+m} \mathbf{s}_{22}^{n,m-1}$ ,  $\mathbf{B} \equiv \mathbf{I} - \mathbf{s}_{22}^{n,m-1} \mathbf{S}_{11}^{n+m}$ , and  $\mathbf{I}$  is an identity matrix. Both matrices  $\mathbf{A}$  and  $\mathbf{B}$  remain non singular for any finite thick stack and they will not introduce poles into the  $\mathbf{s}$ -matrix. For piezoelectric layers, we have derived an expression for the matrix  $\mathbf{S}^n$  defined by Eq.(1) as [14]

$$\mathbf{S}^n = \begin{bmatrix} (\mathbf{e}_n^I)^{-1} \mathbf{R}_n^{11} \mathbf{e}_n^D & (\mathbf{e}_n^I)^{-1} \mathbf{R}_n^{12} \\ \mathbf{R}_n^{21} \mathbf{e}_n^D & \mathbf{R}_n^{22} \end{bmatrix} \quad (4)$$

where  $\mathbf{e}^x \equiv \mathbf{v}^x e^{-j\omega s_2^x h} (\mathbf{v}^x)^{-1}$ , ( $x=D, I$ ),  $\mathbf{v}^D = \mathbf{Q}^{21}$ ,  $\mathbf{v}^I = \mathbf{Q}^{22}$ ,  $\mathbf{s}_2^D \equiv \mathbf{s}_2^{11}$  and  $\mathbf{s}_2^I \equiv \mathbf{s}_2^{22}$ , and  $h$  is the layer thickness, all referring to the layer  $n$ .  $\mathbf{Q}^{ij}$  and  $\mathbf{s}_2^{ij}$  ( $i, j=1, 2$ ) are sub-matrices of the full modal ( $\mathbf{Q}$ ) and diagonal spectral ( $\mathbf{s}_2$ ) matrices relevant to the material eigen-solutions calculated as a function of the longitudinal slowness  $s_1 \equiv k_1/\omega$  parallel to the  $x_1$ -axis, and arranged appropriately [16].  $\mathbf{R}_n^{ij}$  are expressed in explicit terms of the *characteristic surface impedance matrix* (CSIM) of both layers  $n$  and  $n+1$  as

$$\mathbf{R}_n^{11} = \mathbf{C}^{-1} (\mathbf{G}_{n+1}^D - \mathbf{G}_n^D) \quad (5a)$$

$$\mathbf{R}_n^{12} = \mathbf{C}^{-1} (\mathbf{G}_{n+1}^I - \mathbf{G}_n^I) \quad (5b)$$

$$\mathbf{R}_n^{21} = \mathbf{C}^{-1} (\mathbf{G}_n^I - \mathbf{G}_n^D) \quad (5c)$$

$$\mathbf{R}_n^{22} = \mathbf{C}^{-1} (\mathbf{G}_{n+1}^I - \mathbf{G}_n^I) \quad (5d)$$

with  $\mathbf{C} \equiv \mathbf{G}_n^I - \mathbf{G}_{n+1}^D$ . The symbols  $\mathbf{G}_n^x$  ( $x=D, I$ ) stand for the CSIM of the layer  $n$  and is defined by  $\mathbf{G}_n^x \equiv \mathbf{t}_n^x(\mathbf{v}_n^x)^{-1}$  with  $\mathbf{t}_n^D \equiv \mathbf{Q}_n^{11}$ ,  $\mathbf{t}_n^I \equiv \mathbf{Q}_n^{12}$ ,  $\mathbf{v}_n^D \equiv \mathbf{Q}_n^{21}$  and  $\mathbf{v}_n^I \equiv \mathbf{Q}_n^{22}$ . We remark that  $\mathbf{R}_n^{ij}$  exhibit poles when the matrix  $\mathbf{C}$  is singular.  $\mathbf{C}$  does possess a singularity in configurations pertaining the interface wave - an isolated proper mode, independent of  $fh$ , which exists at the interface of two half spaces satisfying some specific material properties. For an interface separating a solid and the vacuum, this mode certainly exists and is nothing but the free *surface acoustic wave* (SAW).

### 3 Various forms of characteristic functions and reduced systems

The recursive algorithm Eq. (3) was derived without involving the stack BC, which means a stack's GTSM is calculated once for all possible passive surrounding media, that can be specified after the recursions in order to determinate the proper modes. The same is true for obtaining responses to a monochromatic excitation of various kinds on either or both sides. To be definite, we assume from now on that all layers of finite thickness are contained in the stack and, consequently, on either side of the stack only a homogeneous half space can exist which is allowed to be a vacuum or a piezoelectric solid. Let the stack's layers be numbered from  $n=1$  to  $N \geq 2$ , which implies that  $m=N-1$  in Eqs.(2) and (3), and that the top and bottom media take on the number 0 and  $N+1$ , respectively. Any mechanically stress-free or clamped and electrically open or shorted stack surface conditions can be described by the CSIM of a passive external half space. By applying the continuity of the state vector at both external surfaces of the stack, we obtain a global system:

$$\begin{bmatrix} \mathbf{s}_{11}^{1:N-1} & -\mathbf{I} & \mathbf{0} & \mathbf{s}_{12}^{1:N-1}(\mathbf{e}_N^I)^{-1} \\ \mathbf{s}_{21}^{1:N-1} & \mathbf{0} & -\mathbf{I} & \mathbf{s}_{22}^{1:N-1}(\mathbf{e}_N^I)^{-1} \\ \mathbf{G}_0^I - \mathbf{G}_1^D & \mathbf{G}_0^I - \mathbf{G}_1^I & \mathbf{0} & \mathbf{0} \\ \mathbf{0} & \mathbf{0} & (\mathbf{G}_N^D - \mathbf{G}_{N+1}^D)\mathbf{e}_N^D & \mathbf{G}_N^I - \mathbf{G}_{N+1}^D \end{bmatrix} \begin{bmatrix} \mathbf{y}_{D1}^- \\ \mathbf{y}_{I1}^- \\ \mathbf{y}_{DN}^- \\ \mathbf{y}_{IN}^+ \end{bmatrix} = \mathbf{0} \quad (6)$$

In Eq.(6),  $\mathbf{y}_{DN}^-$  instead of  $\mathbf{y}_{DN}^+$  is considered as unknown in order to avoid a potential overflow as  $fh_N \rightarrow \infty$ , which would occur if the factor  $(\mathbf{e}_N^D)^{-1}$  instead of  $\mathbf{e}_N^D$  was present within the system matrix. Non trivial solutions require setting to zero the system determinant, yielding a form of the so-called *characteristic function* whose zeros define the values of  $\omega$ - $\mathbf{k}$  pair for the proper mode solutions. When  $\mathbf{s}^{1:N-1}$  has no poles, the determinant  $\Delta_6$  of Eq.(6) is pole-free because all matrices  $\mathbf{G}_n^x$  are. With piezoelectric solid half spaces,  $\mathbf{G}_0^I$  and  $\mathbf{G}_{N+1}^D$  are the same as  $\mathbf{G}_n^x$  defined after Eq.(5); with a top vacuum,  $\mathbf{G}_0^I = \mathbf{G}_v$ , and with a bottom vacuum,  $\mathbf{G}_{N+1}^D = -\mathbf{G}_v$ .  $\mathbf{G}_v$  is a 4-dimensional null matrix except for the (4,4)-element, which is equal to  $j|s_1|\epsilon_0$  coming from vacuum permittivity-generated electrical fields. The cases of clamped and metallized surfaces are not considered here.

Although the proper modes can be determined by Eq. (6), the involved system matrix size is relatively large, 16

against 8 for the GTSM, or 4 for the surface impedance. When the bottom half space is a piezoelectric solid, the  $\mathbf{s}$ -matrix defined in Eq.(2) can be extended to include it so that  $n$  varies from 1 to  $N+1$  and  $m=N$  in Eq.(3). After substituting  $N$  by  $N+1$  in Eq.(6) and accounting for  $\mathbf{y}_{IN+1}^\pm = \mathbf{0}$  (primary assumption that no inverse modes existent in a bottom half space), we can eliminate successively  $\mathbf{y}_{DN+1}^-$  and  $\mathbf{y}_{I1}^-$  in an adequate (not arbitrary) way to arrive at the most-reduced system without introducing poles:

$$[(\mathbf{G}_0^I - \mathbf{G}_1^D) + (\mathbf{G}_0^I - \mathbf{G}_1^I)\mathbf{s}_{11}^{1:N}] \mathbf{y}_{D1}^- = \mathbf{0} \quad (7a)$$

If the top half space is a piezoelectric solid, a reduced pole-free system similar to Eq.(7a) can be obtained. Considering the total stack matrix  $\mathbf{s}^{0:N-1}$  and  $\mathbf{y}_{D0}^\pm = \mathbf{0}$  in Eq.(6) allows us to obtain

$$[(\mathbf{G}_N^D - \mathbf{G}_{N+1}^D)\mathbf{e}_N^D \mathbf{s}_{22}^{0:N-1}(\mathbf{e}_N^I)^{-1} + (\mathbf{G}_N^I - \mathbf{G}_{N+1}^D)] \mathbf{y}_{IN}^+ = \mathbf{0} \quad (7b)$$

In both cases, only one sub-matrix of the GTSM is involved, and the determinant  $\Delta_7$  from Eq.(7a) or Eq.(7b) introduces no poles in spite of a much reduced system size.

With a free stack (vacuum-surrounded), no way exists to obtain Eq.(7) without introducing poles. More generally, for any external half spaces, we can eliminate the input amplitudes  $\mathbf{y}_{IN}^+$  and  $\mathbf{y}_{D1}^-$  from Eq.(6) to obtain a reduced system for the only output amplitudes:

$$\begin{bmatrix} \mathbf{s}_{11}^{1:N-1} \mathbf{R}_0^{22} - \mathbf{I} & \mathbf{s}_{12}^{1:N-1}(\mathbf{e}_N^I)^{-1} \mathbf{R}_N^{11} \mathbf{e}_N^D \\ \mathbf{s}_{21}^{1:N-1} \mathbf{R}_0^{22} & \mathbf{s}_{22}^{1:N-1}(\mathbf{e}_N^I)^{-1} \mathbf{R}_N^{11} \mathbf{e}_N^D - \mathbf{I} \end{bmatrix} \begin{bmatrix} \mathbf{y}_{I1}^- \\ \mathbf{y}_{DN}^- \end{bmatrix} = \mathbf{0} \quad (8)$$

In Eq.(8),  $\mathbf{R}_0^{22}$  and  $\mathbf{R}_N^{11}$  are those given by Eqs.(5d) and (5a) with  $n=0$  and  $N$ , respectively. When both the top and bottom half spaces are the vacuum and the stack surfaces are electrically open,  $\mathbf{G}_0^I = -\mathbf{G}_{N+1}^D = \mathbf{G}_v$ . The matrix  $\mathbf{C}$  involved in  $\mathbf{R}_0^{22}$  becomes  $\mathbf{C}^- = \mathbf{G}_v - \mathbf{G}_1^D$  and  $\mathbf{C}$  in  $\mathbf{R}_N^{11}$  becomes  $\mathbf{C}^+ = \mathbf{G}_N^I + \mathbf{G}_v$ , cf. Eq.(5).  $\mathbf{C}^\pm$  are singular for some particular values of the slowness  $s_1$ , giving rise to additional poles in the system determinant  $\Delta_8$  of Eq. (8). These poles are associated with the solutions of SAW which would exist at the top (bottom) surface of a bottom (top) half space of the same material as the layer 1 ( $N$ ).

### 4 Numerical features and advantages of the s-matrix formalism

In the previous section, we have shown that the characteristic function can appear in different forms for a given BC problem. Now we show that, though all of these functions give the same proper modes, their numerical behaviors can be radically different. Their numerical features are compared, through examples, for various matrix formalisms and for various forms of the same  $\mathbf{s}$ -matrix. In all numerical examples, the stack is assumed to be made of arbitrarily oriented ZnO and LiNbO<sub>3</sub> materials, and the individual layer thickness to be  $h_n=1 \mu\text{m}$ .

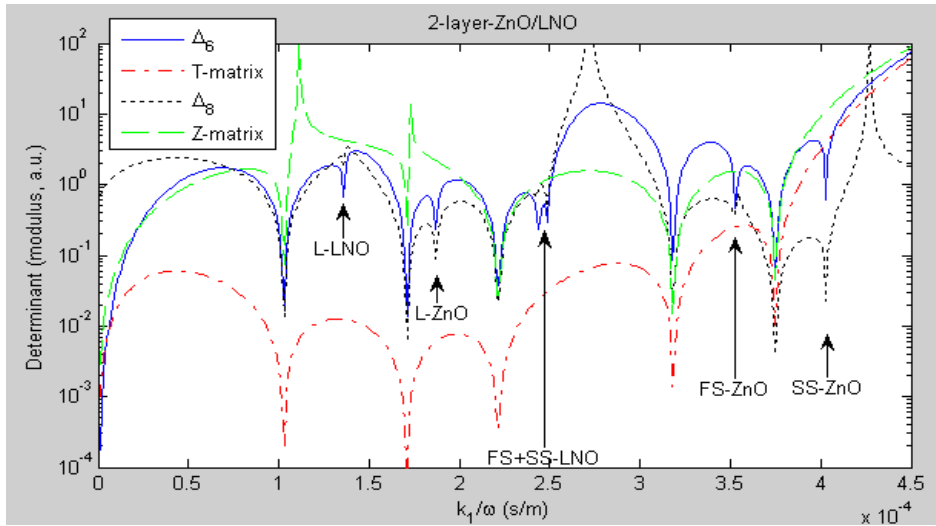


Fig. 1. Four different formalisms for a 2-layer plate of (10,20,30)-ZnO/LNO with  $fh=1000$  m/s. 5 true zeros (plate modes) are common on all curves, 6 pseudo zeros are present in the  $\mathbf{s}$ -matrix formalisms (indicated by arrows at  $s_1=4.03, 3.53,$  and  $1.87$  for the 3 SSBW of ZnO and at  $s_1=2.49, 2.44,$  and  $1.36$  for the 3 SSBW of LNO). The  $\mathbf{Z}$ - and the reduced  $\mathbf{s}$ -matrix by Eq.(8) possess poles.

Figure 1 shows for a 2-layer ZnO/LNO plate and a moderate  $fh=1000$  m/s the characteristic functions obtained by four different formalisms:  $\mathbf{s}$ -matrix via Eqs. (6) and (8),  $\mathbf{Z}$ -, and  $\mathbf{T}$ -matrix. The curve dips represent either true (plate modes) or pseudo zeros (SSBW). We observe 5 true zeros, which are common on all 4 curves, 6 pseudo zeros, 3 for each material, to which only the  $\mathbf{s}$ -matrix is sensible, and 2 poles associated with the  $\mathbf{Z}$ -matrix as well as 2 poles with the  $\mathbf{s}$ -matrix via Eq.(8). With the  $\mathbf{s}$ -matrix,  $\Delta_6$  is pole-free; the poles of  $\Delta_8$  are originated from the SAW modes which would exist at the surface of a half space of ZnO and LNO, respectively. The poles of  $\mathbf{Z}$ -matrix are not due to the SAW modes, but do correspond to plate modes associated with some exotic BC. The  $\mathbf{T}$ -matrix formalism we used is the one involving no inversion of any sub-matrices  $\mathbf{T}_{ij}$  of  $\mathbf{T}$ , i.e.,  $[\mathbf{T}_{11}\mathbf{G}_v+\mathbf{T}_{12}+\mathbf{G}_v(\mathbf{T}_{21}\mathbf{G}_v+\mathbf{T}_{22})]\mathbf{V}_1^{-1}=\mathbf{0}$ , and so is pole-free. Any other forms of the  $\mathbf{T}$ -matrix formalism introduce poles as well. For this moderate  $fh$  value, the superiority of the  $\mathbf{s}$ -matrix over the  $\mathbf{T}$ - and  $\mathbf{Z}$ -matrix is not obvious because the stability issue is not involved and a few poles do not bother much the observation of zeros.

Figure 2 shows results of  $\mathbf{s}$ -matrix formalisms for  $fh=10000$  and 1 m/s, compared with the  $\mathbf{Z}$ -matrix. The  $\mathbf{T}$ -matrix result is not presented due to its instability. The  $\Delta_0$ -like mode tends to SAW in slow ZnO. It manifests as a dip in  $\Delta_6$ -curve, but is not easy to be observed in  $\Delta_8$ -curve. In fact, the SAW-related singularity of  $\Delta_8$ -curve is a zero-pole pair. The  $\mathbf{Z}$ -matrix formalism remains stable, but many poles are present, making it difficult to graphically observe and numerically locate the zeros hidden behind densely displayed poles. The poles arising with the  $\mathbf{Z}$ -matrix are not easy to be removed because the same determinant giving rise to poles possesses also zeros. At extremely low  $fh=1$  m/s, on the other hand, only one plate ( $A_0$ -like) mode exists along with the 6 pseudo zeros due to SSBW, and the  $\mathbf{s}$ -matrix remains stable, as seen in (2,2)-subplot. The position of poles does not vary with the  $fh$  values in Figs. 1 and 2, proving that they are not related to the internal resonant modes. This is in contrast to the  $\mathbf{T}$ -matrix for which the matrix operations-introduced poles appear only above a threshold  $fh$  value, and to the  $\mathbf{Z}$ -matrix for which the exotic BC-related poles depend on  $fh$ .

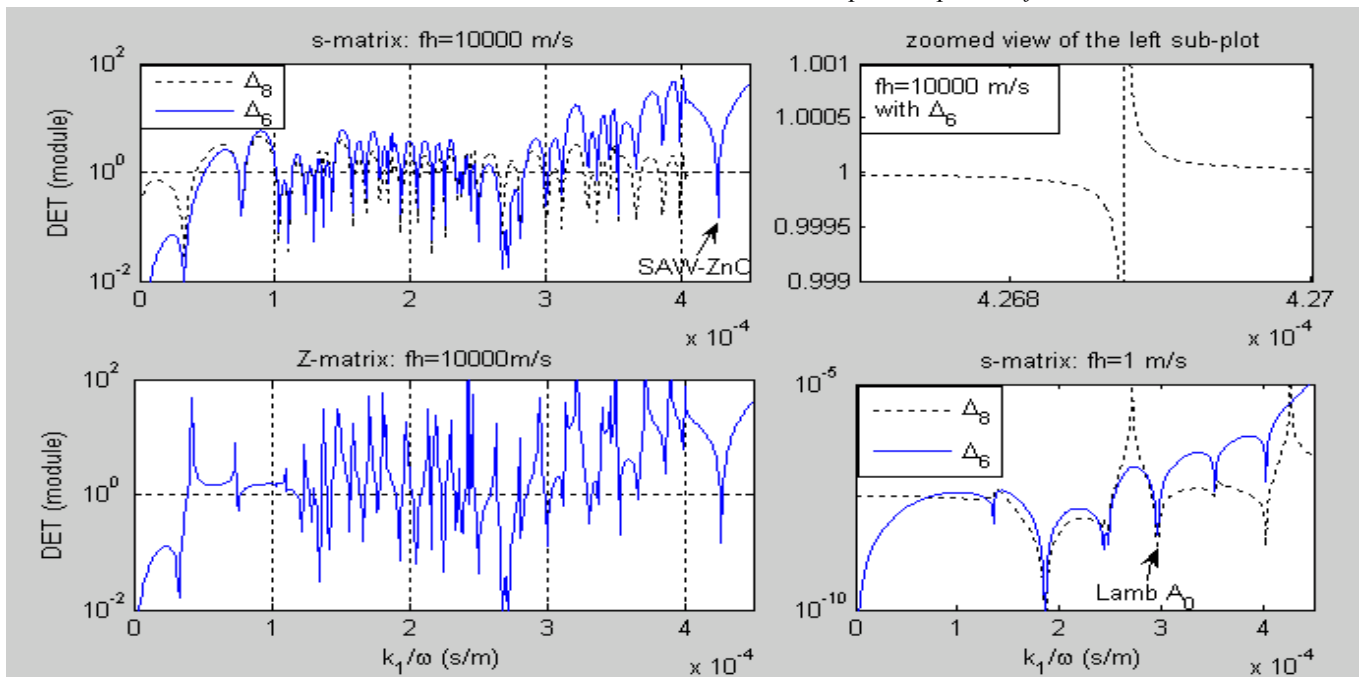


Fig. 2. Same plate as Fig. 1 but for  $fh=10000$  m/s. (1,1)-subplot: plate modes given by  $\mathbf{s}$ -matrix, no poles of  $\Delta_8$  are observed; (1,2)-subplot: zoomed view around  $s_1=4.269e-4$  s/m showing a zero-pole pair of the  $\Delta_8$ -curve; (2,1)-subplot: a lot of poles mixed with zeros by  $\mathbf{Z}$ -matrix; (2,2)-subplot:  $\mathbf{s}$ -matrix remaining stable for extremely low  $fh=1$  m/s; two poles in  $\Delta_8$ -curve are due to SAW in either material of the stack.

Our  $\mathbf{s}$ -matrix formalism also gave successful and spectacular results for  $fh=100000$  m/s [14]. No bad matrix condition was reported by MATLAB during computations of  $\Delta_6$ . 4500 uniform samplings were sufficient for us to well discriminate a total of 310 modes: 2 SAW and 6 SSBW, along with 302 plate modes. At this regime, neither the  $\mathbf{T}$ -nor the  $\mathbf{Z}$ -matrix were able to give a curve having such nice functional features as pole-free, numerically stable, and keeping a rather steady magnitude over the entire interested range of  $s_1$ . With the same ZnO layer but a half space LNO, we obtained 37 quasi-guided modes in ZnO layer between  $s_1=(3.53, 4.03)$ , and 76 true SAW modes between  $s_1=(2.44, 3.53)$ . Some dips between  $s_1=(1.3, 1.9)$  above the cut-off slowness of the slow shear bulk wave of LNO, due to pseudo SAW, were also observed.

Results of a 3-layer ZnO/LNO/ZnO plate for a moderate  $fh=1000$  m/s in Fig. 3 were obtained by using both  $\Delta_6$  and  $\Delta_8$ , along with the results of  $\mathbf{Z}$  and  $\mathbf{T}$  matrices for comparison. We notice that SSBW modes of LNO material are absent, probably because the wave amplitudes of the

middle LNO layer do not appear explicitly in Eqs. (6) and (8). We observe that the  $\mathbf{T}$ -matrix curve grows rapidly with  $s_1$  when some  $s_2$  are complex, which happens even in stable regimes. The growth is especially rapid with high  $fh$ , and this is so with or without a substrate.

Results for the same 3-layer plate but terminated on an additional LNO substrate are given in Fig. 4. The  $\mathbf{T}$ -matrix is compared with 2 different  $\mathbf{s}$ -matrix characteristic functions:  $\Delta_7$  and  $\Delta_{8\text{sub}} \equiv \left| \mathbf{s}_{11}^{1;N-1} \mathbf{R}_0^{22} - \mathbf{I} \right|$  resulted from Eq.(8) with  $\mathbf{y}_{DN}^- = \mathbf{0}$ . As expected,  $\Delta_7$  is pole-free and  $\Delta_{8\text{sub}}$  exhibits a pole originated from the matrix  $\mathbf{R}_0^{22}$  with  $\mathbf{G}_0^I = \mathbf{G}_y$ , due to the SAW mode which would exist at the surface of ZnO half space. Again, the 3 SSBW of ZnO are obvious, but SSBW modes of LNO material are not. We underline that SSBW position keeps unchanged in 2- and 3-layer stacks, with and without a substrate.

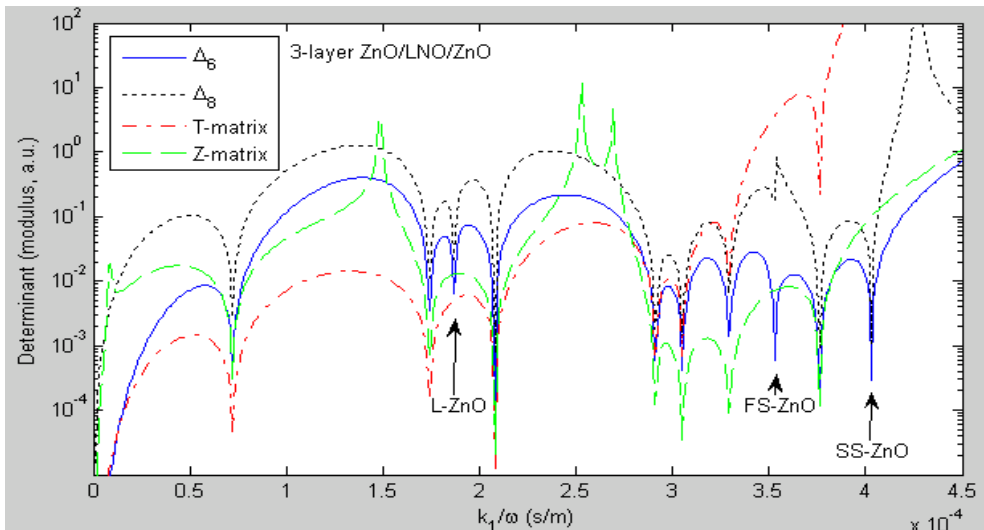


Fig. 3. 3-layer plate with  $fh=1000$  m/s. 7 zeros (plate modes) are common on all curves, only 3 pseudo zeros (SSBW in ZnO, same as in Fig. 1) manifest with the  $\mathbf{s}$ -matrix. Poles are present with the  $\mathbf{Z}$ - and the reduced  $\mathbf{s}$ -matrix via Eq.(8).

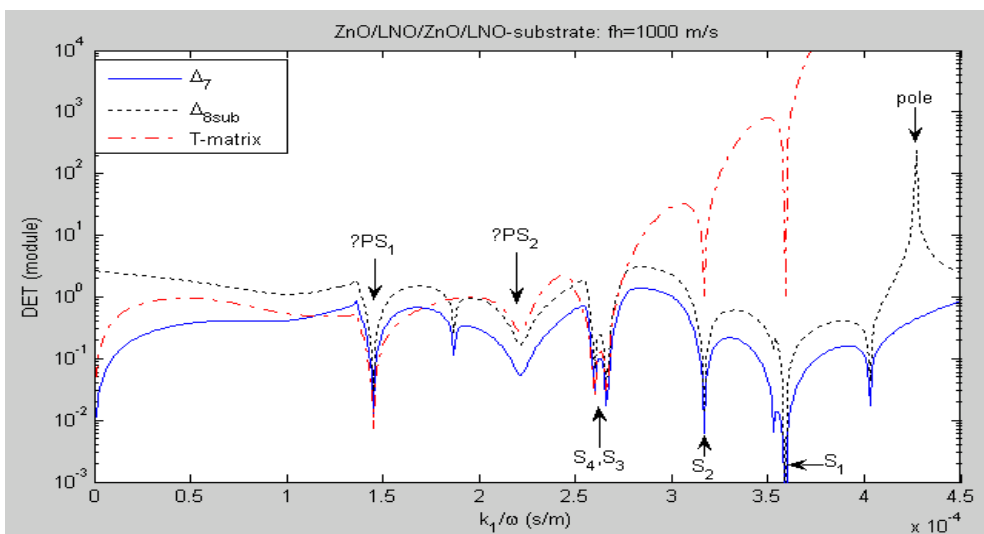


Fig. 4. 3-layer plate (same as Fig. 3) with an additional LNO substrate. The 4 true zeros after 2.54 are true SAW modes (marked  $S_{1,2,3,4}$ ), as clearly shown by the  $\mathbf{T}$ -matrix; ?PS<sub>1,2</sub> indicate 2 pseudo SAW. The curve obtained by modified Eq.(8) exhibits 1 pole. Only observable are 3 SSBW of ZnO, same as in Fig. 3 and not marked.

## 5 Conclusion

The presented comprehensive **s**-matrix approach allows us to analyze easily a layered stack considered alone or in combination with a solid substrate at either or both of its sides, described in terms of its CSIM. Compared with other matrix formalisms, the **s**-matrix provides pole-free characteristic functions, like the **T**-matrix, but does not suffer from the numerical instability even for  $fh=100000$  m/s. Though the **Z**-matrix also gives stable results, the intrinsic poles due to some exotic BC without practical interests trouble the graphic observation and the numerical location of zeros for high  $fh$  values. The reflection **R**-matrix, which is a stable partial **s**-matrix formalism, also suffers from poles, in addition to the need of incorporating the stack BC of the beginning side into the recursions at the outset and repeating the recursions whenever the BC is modified even for the same stack. The total **s**-matrix we developed is the only known formalism that is numerically stable and pole-free. The size-reduced systems we derived in Eq. (7), for stacks surrounded by at least one homogeneous piezoelectric half space, is expected to also be pole-free for most material configurations except for ones where the interfacial wave is pertained. When the stack is surrounded by a vacuum at both sides, any reduced system introduces poles, originating from the SAW solution for a layered half space terminated by a free surface. Another feature of the **s**-matrix resides in its sensitivity to SSBW modes that are usually absent in the **Z**- and **T**-matrix formalisms. The **s**-matrix formalism allows the SAW-like solutions appearing in the extremely high " $fh$ " regime not to be lost by including the wave amplitudes in both the top and bottom layers in the characteristic system, at the price of dealing with 16-dimensional matrices to maximum.

## References

- [1] A. H. Fahmy and E. L. Adler, "Propagation of acoustic waves in multilayers: A matrix description", *Appl. Phys. Lett.*, 20, 495–497 (1973)
- [2] E. L. Adler, "Matrix methods applied to acoustic waves in multilayers," *IEEE Trans. Ultrason., Ferroelect., Freq. Contr.*, 37, 485–490 (1990)
- [3] M. J. S. Lowe, "Matrix techniques for modeling ultrasonic waves in multilayered media", *IEEE Trans. Ultrason., Ferroelect., Freq. Contr.*, 42, 525–542 (1995)
- [4] E. L. Tan, "Hybrid compliance-stiffness matrix method for stable analysis of elastic wave propagation in multi-layered anisotropic media", *J. Acoust. Soc. Am.* 119, 45–53 (2006)
- [5] B. Honein, A. M. B. Braga, P. Barbone, and G. Herrmann, "Wave propagation in piezoelectric layered media with some applications", 1991 *Proc. Conf. Recent Advances Active Contr. Sound Vib.*, 50–63.
- [6] B. Hosten and M. Castaings, "Surface impedance matrices to model the propagation in multilayered media", *Ultrasonics* 41, 501–507 (2003)
- [7] B. Collet, "Recursive surface impedance matrix methods for ultrasonic wave propagation in piezoelectric multilayers", *Ultrasonics* 42, 189–197 (2004)
- [8] S. I. Rokhlin and L. Wang, "Stable recursive algorithm for elastic wave propagation in layered anisotropic media: stiffness matrix method", *J. Acoust. Soc. Am.* 112, 822–834 (2002)
- [9] L. Wang and S. I. Rokhlin, "A compliance/stiffness matrix formulation of general Green's function and effective permittivity for piezoelectric multilayers", *IEEE Trans. Ultrason., Ferroelect., Freq. Contr.* 51, 453–463 (2004)
- [10] B. L. N. Kennett, *Seismic Wave Propagation in Stratified Media*. Cambridge: Cambridge Univ. Press, 1983.
- [11] T. Pastureaud, V. Laude, and S. Ballandras, "Stable scattering matrix method for surface acoustic waves in piezoelectric multilayers," *Appl. Phys. Lett.* 80, 2544–2546 (2002)
- [12] E. L. Tan, "A concise and efficient scattering matrix formalism for stable analysis of elastic wave propagation in multilayered anisotropic solids", *Ultrasonics* 41, 229–236 (2003).
- [13] D. C. Booth, S. Crampin, *The anisotropic reflectivity technique: theory*, *Geophys. J. R. Astron. Soc.* 72, 755–766 (1983)
- [14] V. Y. Zhang and V. Laude, "Unified and stable scattering matrix formalism for acoustic waves in piezoelectric stacks", submitted on Feb. 2008.
- [15] E. L. Tan, "Matrix Algorithms for Modelling Acoustic Waves in Piezoelectric Multilayers", *IEEE Trans. Ultrason., Ferroelect., Freq. Contr.* 54, 2016–2023 (2007)
- [16] V. Zhang, J. E. Lefebvre, C. Bruneel, and T. Gryba, "A unified formalism using effective surface permittivity to study acoustic waves in various anisotropic and piezoelectric multilayers", *IEEE Trans. Ultrason., Ferroelect., Freq. Contr.* 48, 1449–1461 (2001)